INTERNATIONAL JOURNAL FOR NUMERICAL METHODS IN ENGINEERING
Int. J. Numer. Meth. Engng 2001; **52**:1107–1130 (DOI: 10.1002/nme.244)

A meshless method for Kirchhoff plate bending problems

Vitor M. A. Leitão*,†

Departamento de Engenharia Civil, Instituto Superior Técnico, Av Rovisco Pais, 1049-001 Lisboa, Portugal

SUMMARY

In this work a meshless method for the analysis of bending of thin homogeneous plates is presented. This meshless method is based on the use of radial basis functions to build an approximation of the general solution of the partial differential equations governing the Kirchhoff plate bending problem. In order to obtain a symmetric and non-singular linear equation system the Hermite collocation method is used. To assess the formulation a series of plates with different boundary conditions are analysed. Comparisons are made with other results available in the literature. Copyright © 2001 John Wiley & Sons, Ltd.

KEY WORDS: plate bending; meshless method; hermite collocation

1. INTRODUCTION

The use of a mesh (be it domain or boundary one) is a basic characteristic of the traditional approaches for the solution of partial differential equations (PDEs). This is the case for the domain methods (such as the finite difference methods, the finite element methods and the finite volume methods) and also for boundary methods such as the boundary element method. In the first type of methods (the domain ones) assumptions are made for the local approximation which require a mesh to support them. In the case of boundary methods, whereby an integral equation is obtained, a boundary mesh (and, in some cases such as the case of physical nonlinearity, also a domain mesh) is required to obtain a numerical approximation to the boundary integrals involved.

Referring to the dominant approach, the finite element methods, the use of a mesh implies that specific procedures have to be devised just to define the mesh. Also, and to keep the order of the local approximation within reasonable (low) limits, the element size has to be reduced whenever better approximations are pursued.

The extraordinary amount of work which has been put into FEM research since its early days, has, one way or another, circumvented these and other problems associated to the

*Correspondence to: Vitor M. A. Leitão, Departamento de Engenharia Civil, Instituto Superior Técnico, Av. Rovisco Pais, 1049-001 Lisboa, Portugal
†E-mail: vitor@civil.ist.utl.pt

Contract/grant sponsor: PRAXIS XXI; contract/grant number: 2/2.1/CEG/33/94

Received 12 May 2000
Revised 2 May 2001

existence of a mesh and made FEM the dominant approach for most problems in computational mechanics.

Nevertheless, the possibility of obtaining numerical solutions for PDEs without resorting to an element frame, that is a meshless technique, has been the goal of many throughout the computational mechanics community for the past two decades or so.

During this period several procedures have been proposed. It seems that the first work on a meshless method was that of Lucy [1] on smoothed particle hydrodynamics (SPH) which may be considered a precursor to a class of meshless methods of which other representative examples are the works of Nayroles *et al.* [2] on the diffuse element method, the work of Belytschko and co-workers on the element-free Galerkin method [3], the work of Duarte and Oden [4] on the *h–p* clouds, that of Babuska and Melenk [5] on the partition of unity method, and the work of Liu and co-workers on the reproducing kernel method [6]. A good review for this class of meshless methods, which is the one that has produced more results so far, is given in Reference [7].

There are other classes of meshless methods, namely the meshless local boundary equation method and the meshless local Petrov–Galerkin approach of Atluri and Zhu [8], methods based on the use of wavelets (see Reference [9], for example) and methods based on generalized finite differences [10].

Other methods exist for the solution of PDEs which are, inherently, meshless. These are the methods based on the use, as approximating functions, of actual solutions of the governing PDEs by boundary collocation. Reviews on some of these methods, including the Trefftz method [11], the fundamental solutions method, the boundary point collocation method, etc., may be found in References [12, 13]. The work of the author and co-workers on potential problems, plane elasticity and plate bending, see References [14–17], emphasizes the meshless characteristic of the indirect Trefftz collocation approach. The disadvantage of this family of meshless methods is that solutions (trial functions which are solutions of the field equations and, also, particular solutions) must exist so that an approximate solution may be obtained. The requirements on the approximating functions are quite strong and these may be very difficult to devise for a general PDE problem.

It was, basically, the goal of reducing those strong requirements on the approximating functions that lead the author to investigate other meshless techniques that could be more efficiently applied for the solution of general PDEs.

The meshless method being proposed in this work for the analysis of Kirchhoff plate bending relies on the use of radial basis functions (RBFs) and will be described in the following sections.

2. INTERPOLATION USING RBFs

Radial basis functions have initially (early 1970s) been devised by mathematicians, see Hardy [18], working on scattered data fitting and general multi-dimensional data interpolation problems.

The basic idea of scattered data interpolation is described in detail in the works of Kansa [19] and Fasshauer [20], for example.

Assume a set of N points x_i (or nodes) on which interpolation data $f(x_i)$ is known. Assume a set of RBF basis functions (centred at a given number of points which are usually made to

coincide with the x_i points), such as multiquadrics (MQ) $\phi(\|x-x_j\|)=\sqrt{(x-x_j)^2+c_j^2}$ where $x\in\mathbb{R}^d$, and $c_j\neq 0$ is an adjustable parameter that may be seen as a local shape parameter.

An RBF interpolant is assumed in the form of

$$s(x)=\sum_{j=1}^{N}\alpha_j\phi(\|x-x_j\|) \tag{1}$$

which is then solved for the α_j unknowns from the system of N linear equations of the type

$$s(x_i)=f(x_i)=\sum_{j=1}^{N}\alpha_j\phi(\|x_i-x_j\|) \tag{2}$$

In order to ensure the uniqueness of the interpolation a constant, α_{N+1}, is added to the expansion and a constraint on the coefficients is imposed in the form $\sum_{j=1}^{N}\alpha_j=0$.

Multiquadrics (and other members of the infinite class of RBFs such as Gaussians $\exp(-\|x-x_j\|/c_j^2)$ or thin plate splines $\|x-x_j\|\ln\|x-x_j\|$ to name just the most popular ones) are globally supported RBFs in the sense that they are defined over all the domain. There exist also compactly supported RBFs (defined only on parts of the domain) introduced by Wendland [21] and Kansa and Hon [19] which are now receiving increased attention and that may be applied to larger problems than the globally supported RBFs.

3. PDEs SOLUTION USING RBFs

The application of the interpolation technique described above to the analysis of PDEs arising in computational mechanics was first presented by Kansa [22]. In that work an approximate solution is obtained in a form which is very similar to that of expansion (2).

Consider an elliptic PDE (hyperbolic and parabolic PDEs are formulated similarly, see Kansa [19]) with interior LI and boundary LB operators domain:

$$\mathscr{L}u=\mathscr{F} \tag{3}$$

where $\mathscr{L}^{\mathrm{T}}=[\mathrm{LI}\ \ \mathrm{LB}]$ and $\mathscr{F}^{\mathrm{T}}=[\mathrm{FI}\ \ \mathrm{FB}]$ is the right-hand side vector.

Assume an approximation $u_h(X)$ to the PDE in the form, that is, by using radial basis functions:

$$u_h(x)=\sum_{j=1}^{N}\alpha_j\phi(\|x-x_j\|) \tag{4}$$

where $x_j, f_j,\ j=1,\ldots,N$, define a data set.

The unknown coefficients α_j are determined by solving the system of N linear equations formed by applying (that is, by collocating) the operators LI and LB to approximation (4) at N selected points or, better, LI is applied to $N-M$ points and LB is applied to the remaining M points.

$$\mathrm{LI}\,u_h(x_i)=\sum_{j=1}^{N-M}\alpha_j\,\mathrm{LI}\,\phi(\|x_i-x_j\|) \tag{5}$$

$$\mathrm{LB}\, u_h(x_i) = \sum_{j=N-M+1}^{N} \alpha_j \,\mathrm{LB}\, \phi(\|x_i - x_j\|) \tag{6}$$

where LI is applied to $N-M$ points and LB is applied to the remaining points. Again, and in order to ensure the uniqueness of the interpolation a polynomial basis should be added and constraints imposed in a suitable manner which is not considered here for the sake of simplicity.

This form of collocation gives rise to an asymmetric system of equations and is therefore known as the asymmetric collocation method or Kansa's approach.

Fasshauer [23], motivated by previous works on scattered Hermite interpolation, presented a method to obtain an approximate PDE solution which leads to inherently symmetric and non-singular systems of linear equations. This method was also addressed by Wu [24], Franke and Schaback [25] and Jumarhon *et al.* [26].

The basic characteristic of this method is that the operators are applied twice for each pair of collocation point-RBF centre that is being evaluated.

A brief review of the Hermite interpolation, as it appears in Fasshauer [23], is now given. Assume a set of points $x_j,\ j=1,\ldots,N$, a linearly independent set of continuous linear functionals, $\mathscr{L}^{\mathrm{T}} = [L_1,\ldots,L_N]$ and a set of values $L_j f$ constituting the right-hand side vector $\mathscr{F}^{\mathrm{T}} = [F_1,\ldots,F_N]$. The goal is to find an interpolant of the form

$$s(x) = \sum_{k=1}^{N} \alpha_k L_k^{\varepsilon} \phi(\|x - \varepsilon\|) \tag{7}$$

where x is a generic point and ε represents a set of centres for the radial basis functions (which will be from now on considered to coincide with the x points) by satisfying

$$L_j s = L_j f, \quad j = 1,\ldots,N \tag{8}$$

at all points $x_j,\ j=1,\ldots,N$.

Here the following definitions are used:

- $L_k g(x) := (Lg(x))|_{x=x_k}$,
- $L_k^{\varepsilon} g(\|x-\varepsilon\|)$ is the function of x, obtained when L acts on $g(\|x-\varepsilon\|)$ as a function of ε and then evaluated at $\varepsilon = \varepsilon_k$.

The unknowns α_k in expansion (7) are obtained by satisfying (8) and this leads to the system of equations

$$\mathbf{A}\alpha = \mathscr{F} \tag{9}$$

where the elements of matrix $\mathbf{A}$ are of the type

$$A_{jk} = L_j^x L_k^{\varepsilon} g(\|x-\varepsilon\|), \quad j,k = 1,\ldots,N \tag{10}$$

and $L_j^x g(\|x-\varepsilon\|)$ is the function of ε, obtained when L acts on $g(\|x-\varepsilon\|)$ as a function of x and then evaluated at $x = x_j$.

The transposition of the above expressions to the analysis of PDEs is immediate. The following approximation may be considered:

$$u_h(x) = \sum_{k=1}^{N-M} \alpha_k \, \mathrm{LI}_k^{\varepsilon} \, \phi(\|x - \varepsilon_k\|) + \sum_{k=N-M+1}^{N} \alpha_k \, \mathrm{LB}_k^{\varepsilon} \, \phi(\|x - \varepsilon_k\|) \tag{11}$$

where N is the total number of collocation points, M is the number of boundary collocation points, LI and LB are, respectively, the interior and boundary differential operators (which may vary from point to point).

The unknown coefficients α_j are determined by solving the system of N linear equations formed by applying the operators $\mathscr{L}$ to approximation (7) at N selected points:

$$\mathrm{LI}_j^x \, u_h(x_j) = \sum_{k=1}^{N-M} \alpha_k \, \mathrm{LI}_j^x \, \mathrm{LI}_k^{\varepsilon} \, \phi(\|x_j - \varepsilon_k\|) + \sum_{k=N-M+1}^{N} \alpha_k \, \mathrm{LI}_j^x \, \mathrm{LB}_k^{\varepsilon} \, \phi(\|x_j - \varepsilon_k\|) \tag{12}$$

for the interior collocation points and

$$\mathrm{LB}_j^x \, u_h(x_j) = \sum_{k=1}^{N-M} \alpha_k \, \mathrm{LB}_j^x \, \mathrm{LI}_k^{\varepsilon} \, \phi(\|x_j - \varepsilon_k\|) + \sum_{k=N-M+1}^{N} \alpha_k \, \mathrm{LB}_j^x \, \mathrm{LB}_k^{\varepsilon} \, \phi(\|x_j - \varepsilon_k\|) \tag{13}$$

for the boundary collocation points.

This form of collocation gives rise to a symmetric system of equations and is therefore known as the symmetric or Hermite collocation method. The main advantage of this form of collocation when compared to the asymmetric one is that the symmetric system matrix is guaranteed to be invertible, see Fasshauer [23], and that is not the case, at least for some configurations of centres, for the asymmetric one as was proved by Hon and Schabak [27].

As for any numerical technique, the issues of existence and convergence of the solution are of utmost importance. It is, therefore, important to point out that Franke and Schaback [25] have proved that the symmetric collocation method converges with a rate of at least the order of the RBF interpolation minus the order of the differential operator in the PDE.

There are several other issues concerning the use of RBFs for the solution of PDEs that are now being investigated such as compactly supported RBFs, variational approaches (Galerkin) using RBFs, multilevel methods and smoothing, collocation-free global optimization, solvers, preconditioners, domain decomposition, etc.

The work presented herein focus on the application of the symmetric collocation using RBFs for the analysis of Kirchhoff plate bending problems.

4. KIRCHHOFF PLATE BENDING THEORY

Consider the general thin plate represented in Figure 1 where **n** and **t** are the unit normal and tangential vectors, respectively, to the middle plane of the plate.

The differential equation of the deflection surface of an homogeneous, isotropic, arbitrary thin plate under bending is the well-known Lagrange equation:

$$\nabla^4 w = \frac{p}{D} \tag{14}$$

where w is the deflection of the middle surface of the plate, ∇^4 is the biharmonic operator and $D = Et^3/12(1 - \nu^2)$ is the flexural rigidity of the plate.

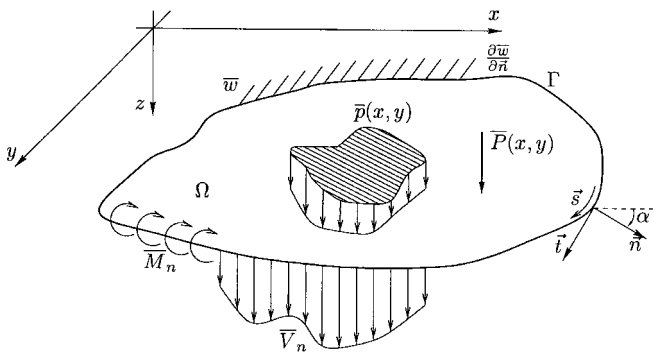

Figure 1. Thin plate and notation.

By neglecting the effect of deformation due to the shear stresses it is possible to identify the dependency between an additional shear force, Q'_n and $\partial M_{nt}/\partial s$ (the derivative of the twisting moment per unit length of a section of a plate normal to direction n).

Thus, for each point on the boundary, two, of the following four, boundary conditions have to be satisfied:

$$w = \bar{w} \tag{15}$$

$$\frac{\partial w}{\partial n} = \frac{\partial \bar{w}}{\partial n} \tag{16}$$

$$M_n = \bar{M}_n \tag{17}$$

$$Q_n + \frac{\partial M_{nt}}{\partial s} = \bar{V}_n \tag{18}$$

where M_n is the bending moment per unit length of a section of a plate perpendicular to n direction, Q_n is the shearing force parallel to z-axis per unit length of section of a plate perpendicular to n direction and $V_n = Q_n + \partial M_{nt}/\partial s$ is the effective shear force parallel to the z-axis of a section of a plate perpendicular to n direction.

It should be noted that at each point on the boundary only the displacement (rotation) or the effective shear force (bending moment) may be imposed but not both simultaneously.

The boundary conditions (16)–(18) may also be expressed in terms of the deflection w as follows:

Normal slope:

$$\frac{\partial w}{\partial n} = \frac{\partial w}{\partial x}\frac{\mathrm{d}x}{\mathrm{d}n} + \frac{\partial w}{\partial y}\frac{\mathrm{d}y}{\mathrm{d}n} = \frac{\partial w}{\partial x}\cos\alpha + \frac{\partial w}{\partial y}\sin\alpha \tag{19}$$

Normal bending moment:

$$M_n = -D\left\{\nu\nabla^2 w + (1-\nu)\left(\cos^2\alpha\frac{\partial^2 w}{\partial x^2} + \sin^2\alpha\frac{\partial^2 w}{\partial y^2} + \sin 2\alpha\frac{\partial^2 w}{\partial x \partial y}\right)\right\} \tag{20}$$

Normal effective shear:

$$V_n = -D\left\{\cos\alpha\frac{\partial}{\partial x}\nabla^2 w + \sin\alpha\frac{\partial}{\partial y}\nabla^2 w + (1-\nu)\frac{\partial}{\partial t}\left[\cos 2\alpha\frac{\partial^2 w}{\partial x\partial y} + \frac{1}{2}\sin 2\alpha\left(\frac{\partial^2 w}{\partial y^2} - \frac{\partial^2 w}{\partial x^2}\right)\right]\right\} \tag{21}$$

where $\partial/\partial t = -\sin\alpha\partial/\partial x + \cos\alpha\partial/\partial y$.

Once the displacement field is known it is straightforward to evaluate the shear forces, the bending and the twisting moments:

$$M_x = -D\left(\frac{\partial^2 w}{\partial^2 x} + \nu\frac{\partial^2 w}{\partial^2 y}\right) \tag{22a}$$

$$M_y = -D\left(\frac{\partial^2 w}{\partial^2 y} + \nu\frac{\partial^2 w}{\partial^2 x}\right) \tag{22b}$$

$$M_{xy} = M_{yx} = -D(1-\nu)\left(\frac{\partial^2 w}{\partial x\partial y}\right) \tag{22c}$$

and

$$Q_x = -D\frac{\partial}{\partial x}\nabla^2 w \tag{23a}$$

$$Q_y = -D\frac{\partial}{\partial y}\nabla^2 w \tag{23b}$$

5. THE RBF SYMMETRIC COLLOCATION FOR KIRCHHOFF PLATES

As described in the previous section the problem to be solved is that of a PDE of the type

$$\nabla^4 w = \frac{p}{D} \tag{24}$$

subjected to the boundary conditions:

$$w = \bar{w}$$

$$\frac{\partial w}{\partial x}\cos\alpha + \frac{\partial w}{\partial y}\sin\alpha = \frac{\partial \bar{w}}{\partial n}$$

$$-D\left\{\nu\nabla^2 w + (1-\nu)\left(\cos^2\alpha\frac{\partial^2 w}{\partial x^2} + \sin^2\alpha\frac{\partial^2 w}{\partial y^2} + \sin 2\alpha\frac{\partial^2 w}{\partial x\partial y}\right)\right\} = \bar{M}_n$$

$$-D\left\{\cos\alpha\frac{\partial}{\partial x}\nabla^2 w+\sin\alpha\frac{\partial}{\partial y}\nabla^2 w\right.$$
$$\left.+(1-\nu)\frac{\partial}{\partial t}\left[\cos 2\alpha\frac{\partial^2 w}{\partial x\partial y}+\frac{1}{2}\sin 2\alpha\left(\frac{\partial^2 w}{\partial y^2}-\frac{\partial^2 w}{\partial x^2}\right)\right]\right\}=\bar{V}_n$$

It should be pointed out that at each boundary point only two of the above boundary conditions may be applied.

These expressions may be rewritten as

$$\mathscr{L}w=\mathscr{F} \tag{25}$$

where

$$\mathscr{L}=\begin{vmatrix}L_{\nabla^4}\\L_w\\L_{\theta_n}\\L_{M_n}\\L_{V_n}\end{vmatrix}=\begin{vmatrix}\nabla^4\\I\\\dfrac{\partial}{\partial x}\cos\alpha+\dfrac{\partial}{\partial y}\sin\alpha\\-D\left\{\nu\nabla^2+(1-\nu)\left(\cos^2\alpha\dfrac{\partial^2}{\partial x^2}+\sin^2\alpha\dfrac{\partial^2}{\partial y^2}+\sin 2\alpha\dfrac{\partial^2}{\partial x\partial y}\right)\right\}\\-D\left\{\cos\alpha\dfrac{\partial}{\partial x}\nabla^2+\sin\alpha\dfrac{\partial}{\partial y}\nabla^2\right.\\\left.+(1-\nu)\dfrac{\partial}{\partial t}\left[\cos 2\alpha\dfrac{\partial^2}{\partial x\partial y}+\dfrac{1}{2}\sin 2\alpha\left(\dfrac{\partial^2}{\partial y^2}-\dfrac{\partial^2}{\partial x^2}\right)\right]\right\}\end{vmatrix} \tag{26}$$

and the right-hand side vector $\mathscr{F}$ is

$$\mathscr{F}=\begin{vmatrix}F_{\nabla^4}\\F_w\\F_{\theta_n}\\F_{M_n}\\F_{V_n}\end{vmatrix}=\begin{vmatrix}\dfrac{p}{D}\\\bar{w}\\\dfrac{\partial\bar{w}}{\partial n}\\\bar{M}_n\\\bar{V}_n\end{vmatrix} \tag{27}$$

By using RBFs an approximation to w, the deflection, may be obtained in the form

$$w_h(\mathbf{x})=\sum_{k=1}^{N_{\nabla^4}}\alpha_k L^{\varepsilon}_{\nabla^4,k}\phi(\|\mathbf{x}-\varepsilon_k\|)+\sum_{k=N_{\nabla^4}+1}^{N_{\nabla^4}+N_w}\alpha_k L^{\varepsilon}_{w,k}\phi(\|\mathbf{x}-\varepsilon_k\|)+\sum_{k=N_{\nabla^4}+N_w+1}^{N_{\nabla^4}+N_w+N_{\theta_n}}\alpha_k L^{\varepsilon}_{\theta_n,k}\phi(\|\mathbf{x}-\varepsilon_k\|)$$
$$+\sum_{k=N_{\nabla^4}+N_w+N_{\theta_n}+1}^{N_{\nabla^4}+N_w+N_{\theta_n}+N_{M_n}}\alpha_k L^{\varepsilon}_{M_n,k}\phi(\|\mathbf{x}-\varepsilon_k\|)+\sum_{k=N_{\nabla^4}+N_w+N_{\theta_n}+N_{M_n}+1}^{N_{\nabla^4}+N_w+N_{\theta_n}+N_{M_n}+N_{V_n}}\alpha_k L^{\varepsilon}_{V_n,k}\phi(\|\mathbf{x}-\varepsilon_k\|) \tag{28}$$

where $\mathbf{x}$ represents the generic position in the co-ordinate system, ε_k represents a given collocation point, the total number of collocation points, distributed randomly or according to

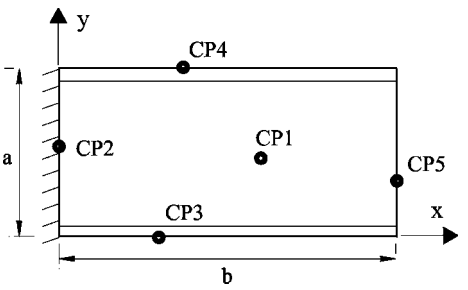

Figure 2. Distribution of collocation points.

some rule on the domain and boundary, is N, N_{∇^4} is the number of points where the field equation (14) is enforced and N_w, N_{θ_n}, N_{M_n} and N_{V_n} are, respectively, the number of points where boundary conditions (15)–(18) are imposed.

In this work the multiquadrics RBF are used, that is, $\phi(\|\mathbf{x}-\mathbf{x}_j\|)=\sqrt{(\mathbf{x}-\mathbf{x}_j)^2+c_j^2}$ where c_j is constant for all points.

The deflection approximation is known as soon as all the α_j coefficients are determined. In order to achieve that, a system of linear equations $\mathscr{L}w=\mathscr{F}$ has to be defined by collocating (that is, by applying the appropriate differential operator) at each interior or boundary collocation point (CP).

To illustrate the application of the technique let us consider the rectangular plate represented in Figure 2, loaded uniformly and subjected to different types of boundary conditions, namely, one side is clamped, two sides are simply supported and the remaining one is free.

Consider, for the sake of simplicity, that there is only one collocation point per side and only one interior collocation point. The numbering is shown in Figure 2.

At each CP the appropriate condition(s) must be enforced:

- CP1, is an interior point and therefore only operator L_{∇^4} must be applied. Notice that the operator is applied as a function of the first variable, the collocation point, and not that of the second variable, the RBF centre.
- CP2, is a boundary point. The boundary conditions on this edge of the plate are $w|_{0,y}=0$ and $\partial w/\partial n|_{0,y}=0$, that is, the edge is clamped. Both conditions (besides the governing differential operator L_{∇^4}) must be imposed at the same geometric position, CP2. In fact, each boundary collocation point is a triple point in the sense that three different operators have to be applied at that single geometric point. Therefore, L_{∇^4}, L_w and L_{θ_n} must be applied at CP.
- CP3, is a boundary point. The boundary conditions on this edge of the plate are $w|_{x,0}=0$ and $M_n|_{x,0}=0$, that is, the edge is simply supported. Therefore, L_{∇^4}, L_w and L_{M_n} must be applied at CP3.
- CP4, is a boundary point. The boundary conditions on this edge of the plate are $w|_{x,a}=0$ and $M_n|_{x,a}=0$, that is, the edge is simply supported. Therefore, L_{∇^4}, L_w and L_{M_n} must be applied at CP4.
- CP5, is a boundary point. The boundary conditions on this edge of the plate are $M_n|_{b,y}=0$ and $V_n|_{b,y}=0$, that is, a free edge. Therefore, L_{∇^4}, L_{M_n} and L_{V_n} must be applied at CP5.

The first row of the coefficient matrix (representing the system of linear equations) is nothing else than the application of operator L_{∇^4} on CP1 as a function of the first argument $\mathbf{x}$ of the RBF to approximation (28):

$$\begin{aligned} L_{\nabla^4} w_h(\mathbf{x_1}) = & \sum_{k=1}^{N_{\nabla^4}} \alpha_k L^x_{\nabla^4} L^{\varepsilon}_{\nabla^4,k} \phi(\|\mathbf{x_1} - \varepsilon_k\|) + \sum_{k=N_{\nabla^4}+1}^{N_{\nabla^4}+N_w} \alpha_k L^x_{\nabla^4} L^{\varepsilon}_{w,k} \phi(\|\mathbf{x_1} - \varepsilon_k\|) \\ & + \sum_{k=N_{\nabla^4}+N_w+1}^{N_{\nabla^4}+N_w+N_{\theta_n}} \alpha_k L^x_{\nabla^4} L^{\varepsilon}_{\theta_n,k} \phi(\|\mathbf{x_1} - \varepsilon_k\|) \\ & + \sum_{k=N_{\nabla^4}+N_w+N_{\theta_n}+1}^{N_{\nabla^4}+N_w+N_{\theta_n}+N_{M_n}} \alpha_k L^x_{\nabla^4} L^{\varepsilon}_{M_n,k} \phi(\|\mathbf{x_1} - \varepsilon_k\|) \\ & + \sum_{k=N_{\nabla^4}+N_w+N_{\theta_n}+N_{M_n}+1}^{N_{\nabla^4}+N_w+N_{\theta_n}+N_{M_n}+N_{V_n}} \alpha_k L^x_{\nabla^4} L^{\varepsilon}_{V_n,k} \phi(\|\mathbf{x_1} - \varepsilon_k\|) \end{aligned} \tag{29}$$

The second row of the coefficient matrix is the application of operator L_w on CP2 as a function of the first argument $\mathbf{x}$ of the RBF:

$$\begin{aligned} L_w w_h(\mathbf{x_2}) = & \sum_{k=1}^{N_{\nabla^4}} \alpha_k L^x_w L^{\varepsilon}_{\nabla^4,k} \phi(\|\mathbf{x_2} - \varepsilon_k\|) + \sum_{k=N_{\nabla^4}+1}^{N_{\nabla^4}+N_w} \alpha_k L^x_w L^{\varepsilon}_{w,k} \phi(\|\mathbf{x_2} - \varepsilon_k\|) \\ & + \sum_{k=N_{\nabla^4}+N_w+1}^{N_{\nabla^4}+N_w+N_{\theta_n}} \alpha_k L^x_w L^{\varepsilon}_{\theta_n,k} \phi(\|\mathbf{x_2} - \varepsilon_k\|) \\ & + \sum_{k=N_{\nabla^4}+N_w+N_{\theta_n}+1}^{N_{\nabla^4}+N_w+N_{\theta_n}+N_{M_n}} \alpha_k L^x_w L^{\varepsilon}_{M_n,k} \phi(\|\mathbf{x_2} - \varepsilon_k\|) \\ & + \sum_{k=N_{\nabla^4}+N_w+N_{\theta_n}+N_{M_n}+1}^{N_{\nabla^4}+N_w+N_{\theta_n}+N_{M_n}+N_{V_n}} \alpha_k L^x_w L^{\varepsilon}_{V_n,k} \phi(\|\mathbf{x_2} - \varepsilon_k\|) \end{aligned} \tag{30}$$

The third row of the coefficient matrix is the application of operator L_{θ_n} on CP2 as a function of the first argument $\mathbf{x}$ of the RBF:

$$\begin{aligned} L_{\theta_n} w_h(\mathbf{x_2}) = & \sum_{k=1}^{N_{\nabla^4}} \alpha_k L^x_{\theta_n} L^{\varepsilon}_{\nabla^4,k} \phi(\|\mathbf{x_2} - \varepsilon_k\|) + \sum_{k=N_{\nabla^4}+1}^{N_{\nabla^4}+N_w} \alpha_k L^x_{\theta_n} L^{\varepsilon}_{w,k} \phi(\|\mathbf{x_2} - \varepsilon_k\|) \\ & + \sum_{k=N_{\nabla^4}+N_w+1}^{N_{\nabla^4}+N_w+N_{\theta_n}} \alpha_k L^x_{\theta_n} L^{\varepsilon}_{\theta_n,k} \phi(\|\mathbf{x_2} - \varepsilon_k\|) \\ & + \sum_{k=N_{\nabla^4}+N_w+N_{\theta_n}+1}^{N_{\nabla^4}+N_w+N_{\theta_n}+N_{M_n}} \alpha_k L^x_{\theta_n} L^{\varepsilon}_{M_n,k} \phi(\|\mathbf{x_2} - \varepsilon_k\|) \\ & + \sum_{k=N_{\nabla^4}+N_w+N_{\theta_n}+N_{M_n}+1}^{N_{\nabla^4}+N_w+N_{\theta_n}+N_{M_n}+N_{V_n}} \alpha_k L^x_{\theta_n} L^{\varepsilon}_{V_n,k} \phi(\|\mathbf{x_2} - \varepsilon_k\|) \end{aligned} \tag{31}$$

The other rows of the system matrix are obtained in the same way which leads to a total of 13 equations to be solved for the 13 unknown α coefficients.

5.1. Particular solutions

In order to analyse other types of loading than simply the case of uniform load it is necessary to consider the use of particular solutions.

The particular solution for a concentrated load, $\bar{P}$, acting on (x_P, y_P), is given by

$$\overset{\circ}{w} = \frac{\bar{P}}{8\pi D} r_P^2 \ln r_P \tag{32}$$

where $r_P^2 = (x - x_P)^2 + (y - y_P)^2$ and

$$\lim_{r_P \to 0} \overset{\circ}{w} = 0$$

For general types of loading it is possible to use the solution for a concentrated load and integrate it over a given region to obtain its effect in terms of transversal displacements (deflections) after which all other fields may be derived.

6. IMPLEMENTATION ASPECTS

Collocation techniques are always less demanding in terms of computational effort than techniques based on integrations of residues along the boundary and/or in the domain such as with finite element, boundary element methods or other Galerkin-type regular boundary formulations (non collocation Trefftz techniques or similar), see Reference [28].

The formulation here described has the added advantage that it leads to a symmetric system of linear equations. As can be seen in a previous work by the author [29] most of the CPU time required for the analysis of a given PDE by using collocation (an indirect Trefftz formulation leading to a non-symmetric matrix) is, in fact, at the solution stage whereas for Galerkin-type Trefftz techniques (leading to symmetric matrices) the assembling or the matrix creation is what takes longer.

The technique here presented for plate bending is, therefore, very efficient in what concerns CPU usage for creating and solving the system of linear equations.

The drawback is the need to actually code all the combined operators required to create each entry $A_{jk} = L^x_{\theta_n} L^{\varepsilon}_{V_n} \phi(\|x_j - \varepsilon_k\|)$ in the system matrix $\mathbf{A}$.

By using a symbolic mathematics software, Mathematica [30], this task is made quite simple.

The definition of the number and the distribution of the collocation points (which are made to coincide with the RBF centres) is, of course, an important issue since it affects the quality of the approximation.

A sufficient number of points must exist along the boundary as it is on the boundary that stronger variations of the static variables occur. As a rule of thumb at least four points should be used at each edge. As to what concerns the position of such points, a regular distribution of points along the boundary, does not necessarily gives the best answers. In the field of discontinuous boundary elements, it is well known that the optimal position for collocation

corresponds to that of the Gauss points, Parreira [31]. The same conclusions were observed by Zielinski and Herrera [32] in the field of Trefftz techniques.

This form of distribution pushes the points further to the ends of the edges and these locations correspond to areas of the highest variations of the static variables. In some cases, for some geometry and boundary conditions configurations, these may even be areas of singularities which are a problem in itself [17].

Also, a sufficient number of points must be defined in the domain. As for its distribution, there are much more options than for the boundary collocation. Any appropriate number of randomly distributed points should be able to model the problem reasonably well. It should be pointed out that the type of load (especially if it is localized) could determine the number and the position of some of the internal collocation points which should be added just to bring to the system enough information about the load.

In this work only regular distribution of collocation points will be considered. Different strategies for the distribution of collocation points are currently being investigated.

7. NUMERICAL TESTS

The numerical tests here reported concern the cases of circular and square plates subjected to uniformly distributed loads and to concentrated loads. These cases illustrate the use of the proposed technique and the accuracy of the numerical results obtained. Results for rectangular plates are not presented here as many rectangular plates can be analysed as square ones with the proper boundary conditions (namely, for symmetrical loading by imposing the normal slope and the normal effective shear to be zero at the edge on the symmetry axis, and for anti-symmetrical loading by imposing the deflection and the normal bending moment to be zero at the edge on the symmetry axis).

Although these are simple plates (at least in terms of geometry) the formulation is not limited to rectangular or circular shapes. For more general shapes the strategy will be to consider multiple regions and to appropriately match the interface conditions from one region to another. This is what, basically, was done by the author (and co-worker) in a previous work using a Trefftz collocation technique [16, 17] and will be addressed in the near future with the present RBF technique.

The methodology chosen for presenting the results and also the tests conducted follow closely that of Jin *et al.* [33], a reference work for Trefftz formulation (which may also be considered, up to a certain point, meshless). Given the fact that RBF and Trefftz share some features the reproduction of the results obtained by Jin *et al.* [33] was deemed relevant. Amongst those common features are, for example, that both techniques lead to global approximations of the relevant variables in a way which is more closely related than with, generally speaking, finite element methods and that the number of unknowns/equations is usually much lower than that of standard finite element techniques for obtaining similar accuracy.

In order to assess the present formulation the following numerical tests were considered:

1. clamped square plate uniformly loaded;
2. simply supported square plate uniformly loaded;
3. clamped square plate subjected to a concentrated central load;

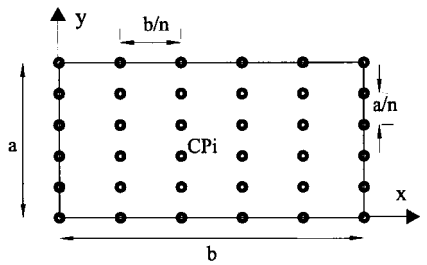

Figure 3. Distribution of collocation points used in the tests on square plates.

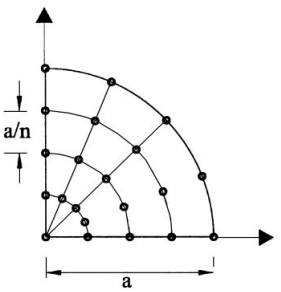

Figure 4. Distribution of collocation points used in the tests on circular plates.

4. uniformly loaded square plate supported only at the corners;
5. clamped circular plate uniformly loaded;
6. simply supported circular plate uniformly loaded;

In all tests the following values were considered: $E = 10920.0$, $v = 0.3$, $a = 1.0$ (characteristic length), $t = a/10$, $\bar{p} = 1.0$ and $\bar{P} = 1.0$.

In all tests on square plates the distribution of collocation points was chosen to be regularly spaced (at distances a/n where n is the number of divisions) both in the domain and along the boundary as represented in Figure 3. Other types of distributions will be addressed in future works. To avoid singularities that may occur at the corners, only the equilibrium condition is enforced there (the corner) for plates where the edges converging to a given corner have different types of boundary conditions. Another alternative would have been to remove the corner points and introduce an extra pair of collocation points at each side of the corner at a small distance from the corner. As will be seen from the results obtained, the chosen approach (removal of the corners without adding extra points) does not oversimplify the model.

The number of positions defined is then $(n+1)^2$. The total number of collocation points may vary depending on whether the corner points are considered or not. The total number of equations also varies but is, in general, $3 \times$ number of boundary collocation points plus the number of internal collocation points.

For the circular plates, of which only a quarter was considered due to symmetry, the distribution of collocation points was chosen to be regularly spaced (at distances a/n where n is the number of divisions) both in the domain and along the boundary as represented in Figure 4.

All the results presented in a tabular form are normalized as defined next:

- $w^{\text{adim}} = w\,D/\bar{p}\,a^4$ or $w^{\text{adim}} = w\,D/\bar{P}\,a^2$;
- $\theta_i^{\text{adim}} = \theta_i\,D/\bar{p}\,a^3$ or $\theta_i^{\text{adim}} = \theta_i\,D/\bar{P}\,a$;
- $M_{ij}^{\text{adim}} = M_{ij}/\bar{p}\,a^2$ or $M_{ij}^{\text{adim}} = M_{ij}/\bar{P}$;
- $Q_i^{\text{adim}} = Q_i/\bar{p}\,a$ or $Q_i^{\text{adim}} = Q_i a/\bar{P}$.

The contour plots or three-dimensional graphs were not normalized as they are shown only to illustrate the way in which the fields vary along the domain.

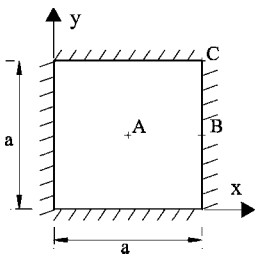

Figure 5. Clamped square plate.

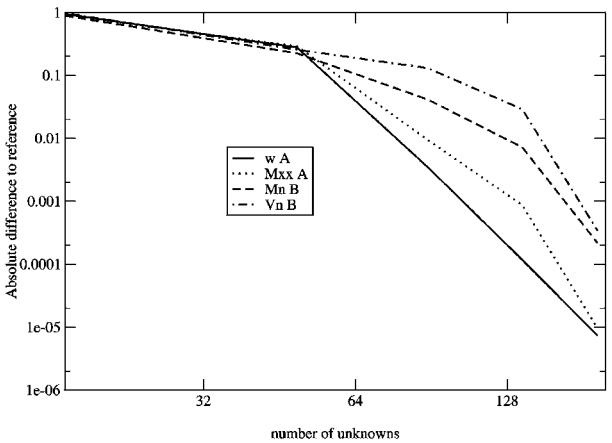

Figure 6. Convergence of the results for the uniformly loaded clamped square plate shown as the absolute differences to those of Reference [33].

Table I. Clamped square plate with uniform load distribution.

	Point A		Point B		
Method	$100\,w^{\text{adim}}$	$10\,M_{xx}^{\text{adim}}$	V_n^{adim}	$10\,M_n^{\text{adim}}$	Reference
HT	0.12653	0.22906	−0.441	−0.513	[35]
TC	0.12653	0.22909		−0.51323	[15]
TDM	0.12653	0.22905	−0.441024	−0.513370	[33]
Compat.	0.126	0.231		−0.513	[34]
RBF	0.1265	0.2291	−0.4412	−0.5135	

HT: One hybrid-Trefftz element with 52 unknowns. TC: Trefftz collocation with 52 unknowns. TDM: 7 quadratic boundary elements per side. RBF: $n = 9$.

7.1. Clamped square plate under uniform load

Consider a uniformly loaded square plate as represented in Figure 5. Timoshenko [34] presents a solution for this case based on the use of the solution for the uniformly loaded simply supported square plate and that of the same plate subjected to moments along the edges so that compatibility is enforced, thus being referred in the tables below as *Compat*. The results he obtained and those of other references are shown in Table I together with the present results. Normalized results are shown for two points (as seen in Figure 5), namely in the middle of the plate-point A, and at the centre of the edge-point B. The representative values at these points are, respectively, the displacement and the bending moment at point A, and the normal shear and the normal moment at point B.

The results obtained with the present technique are all very similar to the results obtained with other approaches. The approaches here chosen to for comparison are all, except the already mentioned Timoshenko [34] solution, based on the Trefftz method.

The Trefftz method consists essentially in using an approximation basis (the T-functions) that solves locally the system of partial differential equations that governs the boundary value modelled to establish an algebraic solving system that enforces consistently the boundary conditions. The main aspects of each of these Trefftz techniques are briefly listed below:

- HT, the hybrid-Trefftz formulation of Jirousek and Leon [35], where, by considering independent boundary and domain approximations (for the relevant fields) a general purpose plate bending element was developed in a way that allows for its integration within a FEM code (that is, a nodal frame is considered).
- TDM, the Trefftz direct method of Jin, Cheung and Zienkiewicz [33], whereby an integral equation is derived in a similar way to that of the boundary element method (that is, by using the Maxwell–Betti reciprocal theorem) but replacing the fundamental solutions by the T-functions.
- TC, the Trefftz collocation method, closely related to the original work of Trefftz [11], where the T-functions are used in the approximation of the variables involved in the boundary conditions (for a given problem) which are then approximately matched.

The approximations Trefftz-type of techniques provide are, mainly due to the use of actual solutions of the governing equations, quite accurate even for a low number of degrees of freedom. The present technique, despite the use of very simple functions which are not, by any means, solutions of the governing equation, does not require many unknowns (degrees of freedom) to attain a relatively good accuracy. The convergence of the results to those of Reference [33] with respect to the number of unknowns, m, is shown in Figure 6. In this test, m takes the values 17, 49, 89, 137 and 193 corresponding to, respectively, 3, 5, 7, 9 and 11 grid divisions. The convergence pattern of the deflection and the bending moment at point A (that is, at the centre of the plate) is more pronounced than that of the normal bending moment and shear at point B which is located at the edge. This result was expected as it is on the boundary that bigger errors occur and this is not a characteristic specific of the present formulation.

A basic feature of the proposed technique, which is the ease to compute and plot any required result, is illustrated by plotting, in Figures 7–9, the deformed shape and the shearing force components for the plate.

Finally, and just to give an idea of how computation time varies with the number of unknowns (that is, the size of the system matrix, m) the number of floating point operations, flops or f, was computed (this is a system function within Matlab, the environment where the formulation was implemented [36]) and plotted against m in Figure 10. The three graphs show the variation of the total number of flops, the number of flops to assemble the system matrix and the number of flops to solve the system. By running a regression analysis it is possible to say that the solving stage is of order $m^{2.81}$, the assembling stage is of order $m^{2.02}$ and the total process is of order $m^{2.42}$. As expected, and similarly to what happens with other collocation techniques [29], as the dimension of the systems grow so grows the time spent solving the system. An iterative solver would, probably, be beneficial.

7.2. Clamped square plate under a central concentrated load

Consider the same clamped square plate as in the previous case now subjected to a concentrated load of magnitude P at point B, that is, the centre of the plate.

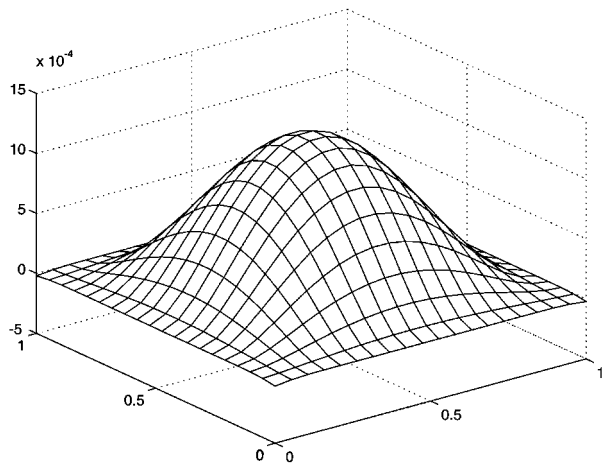

Figure 7. Uniformly loaded clamped square plate: deformed shape.

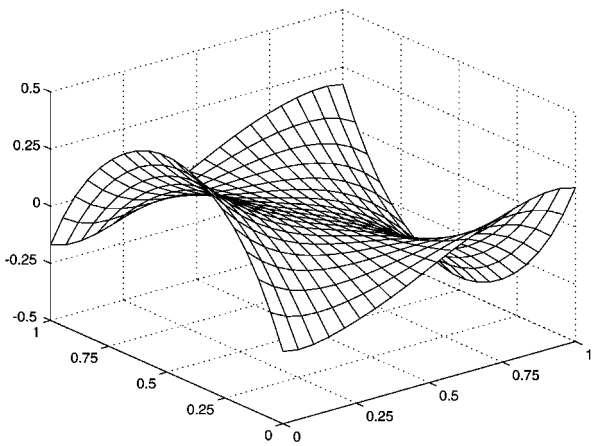

Figure 8. Uniformly loaded clamped square plate: shearing force q_x distribution.

Timoshenko [34] presents a solution for this case based also on the solution for the uniformly loaded simply supported plate and by superposing appropriate states. The results he obtained and those of other references are shown in Table II together with the present results.

As in the previous case the results are very similar to the other references. The convergence pattern is of similar type as well. A contour plot of the twisting moment, m_{xy}, is represented in Figure 11 where is evident the effect of the concentrated load.

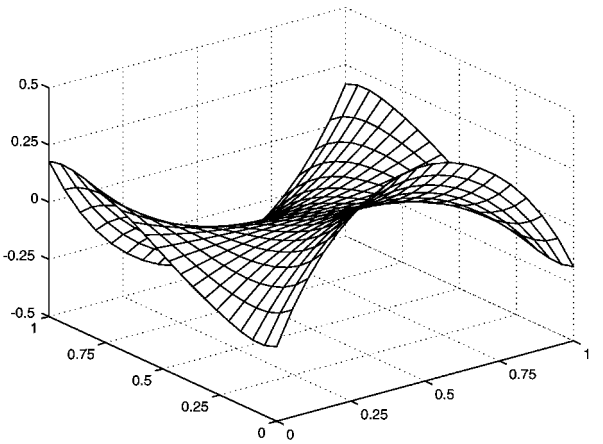

Figure 9. Uniformly loaded clamped square plate: shearing force q_y distribution.

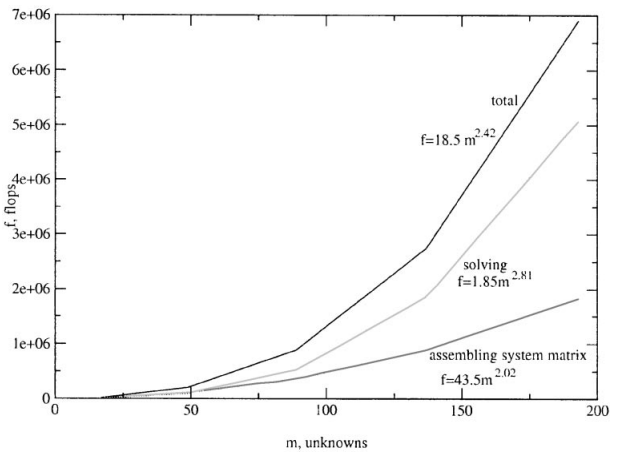

Figure 10. Floating point operations vs number of unknowns.

Table II. Clamped square plate under central concentrated load.

	Point A	Point B	
Method	$100\,w^{\text{adim}}$	$10\,M_{xx}^{\text{adim}}$	Reference
HT	0.56120	−1.258	[35]
TDM	0.56120	−1.25770	[33]
Compat.	0.560	−1.257	[34]
RBF	0.5612	−1.2580	

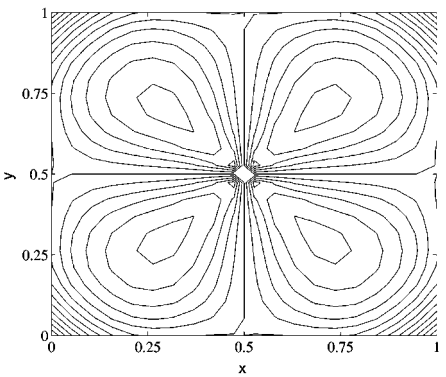

Figure 11. Concentrated load on a clamped square plate: twisting moment, m_{xy}, distribution.

Table III. Simply supported square plate with uniform load distribution.

	Point A		Point B	Point C	
Method	$100\,w^{\text{adim}}$	$10\,M_{xx}^{\text{adim}}$	V_n^{adim}	$10\,(2\|\|M_{xy}^{\text{adim}}\|\|)$	Reference
HT	0.40624	0.478868		0.093	[35]
TC	0.40629	0.47893			[15]
TDM	0.406234	0.478863	−0.420891	0.651655	[33]
Navier	0.4062	0.4789	−0.420	0.6496	[34]
RBF	0.4066	0.4792	−0.4218	0.6432	

7.3. *Simply supported square plate under uniform load*

Consider a uniformly loaded simply supported square plate. This is a case for which there is an exact solution [34] (the Navier series solution) in the form

$$w(x,y)=\frac{16\,pa^4}{\pi^6 D}\sum_{m=1}^{\infty}\sum_{n=1}^{\infty}\frac{\sin(m\pi x/a)\sin(n\pi y/a)}{mn(m^2+n^2)^2} \tag{33}$$

where $m=1,3,5,\ldots$ and $n=1,3,5,\ldots$.

Results obtained by considering 100 terms of the series and those of other references are shown in Table III together with the present results obtained for $n=11$ in each direction.

In Figures 12 and 13 the shearing force components, q_x and q_y, are represented.

7.4. *Uniformly loaded plate supported only at the corners*

Consider a uniformly loaded square plate supported only at the corners.

Timoshenko [34] presents a solution (for $\nu=0.25$ and 0.3) for this case based on the solution for the uniformly loaded plate with four sides supported elastically and taking the limit as the stiffness of the elastic supports goes to zero. In Table IV those results are presented together with the results obtained with the proposed technique for $n=7$, corresponding to 93 equations.

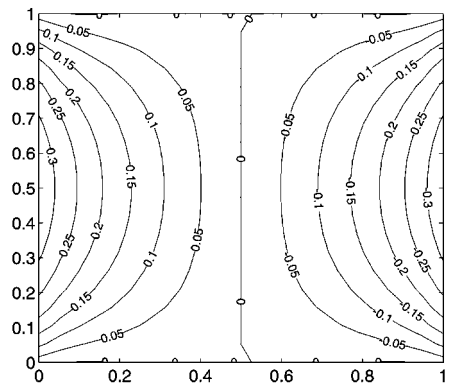

Figure 12. Uniformly loaded simply supported square plate: shearing force q_x distribution.

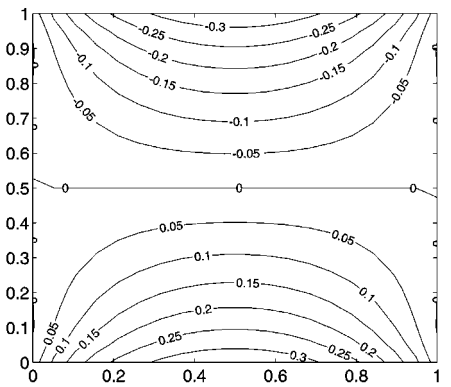

Figure 13. Uniformly loaded simply supported square plate: shearing force q_y distribution.

Table IV. Uniformly loaded plate supported only at the corners.

	Point A		Point B		
Method	$100\,w^{\text{adim}}$	$10\,M_{xx}^{\text{adim}}$	$100\,w^{\text{adim}}$	$10\,M_{xx}^{\text{adim}}$	Reference
Compat. $\nu = 0.25$	0.257	0.1109		0.1527	[34]
RBF $\nu = 0.25$	0.2603	0.1096	0.1766	0.1503	
Compat. $\nu = 0.3$	0.249	0.1090		0.1404	[34]
RBF $\nu = 0.3$	0.2529	0.1111	0.1758	0.1498	

In order to observe the effect of the Poisson's ratio, which Timoshenko [34] says '*has but little influence on the deflections and moments at the centre of the plate*; *its effect on the edge moments is more considerable*', the plate was analysed, with the proposed technique, for a series of values of ν from 0 to 0.3. A finite element model (with 1600 shell elements) was also defined and a commercial finite element code (SAP2000 [37]) was used to carry out the same tests on the effect of the Poisson's ratio on the deflections and moments. These results are represented in Figure 14. In this figure the influence of ν on the bending moments at both points (in the centre of the plate and at the edge) is relatively small. As a matter of fact the biggest influence is seen on the centre point deflection but not even there the results vary significantly. The edge bending moment, which for Timoshenko [34] increases a bit as ν decreases, is, here and also for the FEM, almost flat although very close to Timoshenko's results. Both, the FEM and the proposed technique feature the same trend for all graphs and the differences, which start at around 5 per cent for $\nu = 0$, decrease steadily to around 0.5 per cent for larger values of ν. It should be pointed out that the FEM mesh used here is quite refined (the total number of equations is 10073) and this was intended as to provide a 'good' approximate solution. A coarser mesh (a 10×10 with a total of 710 equations) was also tested and the differences to the present results are, in general, cut by half becoming virtually indistinguishable for larger values of ν.

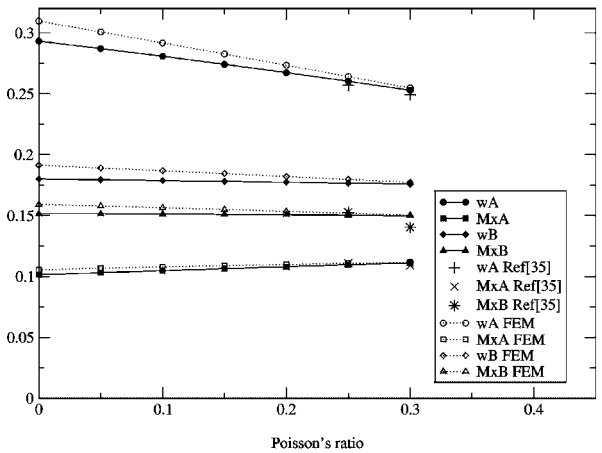

Figure 14. Uniformly loaded square plate supported only at the corners: effect of v.

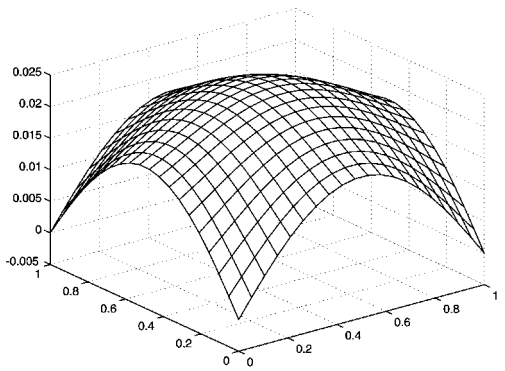

Figure 15. Uniformly loaded square plate supported only at the corners: deformed shape.

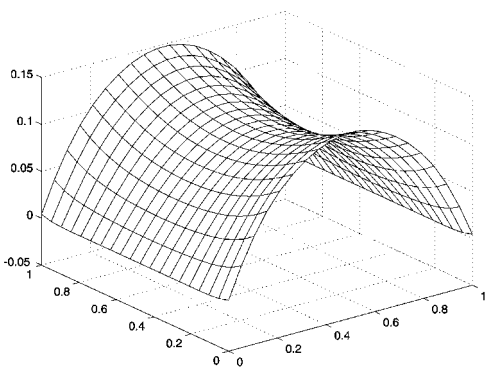

Figure 16. Uniformly loaded square plate supported only at the corners: M_x distribution.

To further illustrate the results obtained a series of plots were made: the deformed shape is represented in Figure 15; the bending moment (the x component only as the y component is, due to symmetry, exactly the same along the y-axis) and the twisting moment are shown in Figures 16 and 17.

7.5. Clamped circular plate under uniform load

Consider a uniformly loaded circular plate of which only a quarter is considered due to symmetry as represented in Figure 18.

Circular plates are usually easier to analyse than rectangular ones. Polar co-ordinates are normally used to obtain exact or approximate solutions for these plates. Timoshenko [34]

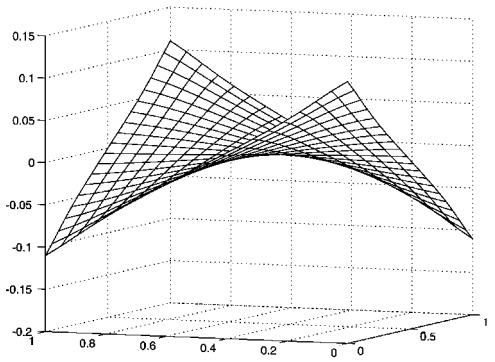

Figure 17. Uniformly loaded square plate supported only at the corners: M_{xy} distribution.

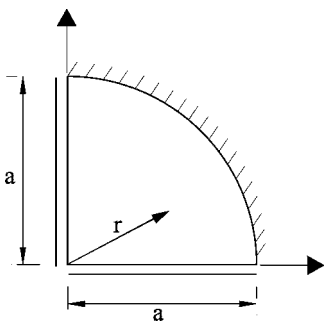

Figure 18. Quarter of a clamped circular plate.

Table V. Clamped circular plate under uniform load.

	Exact		RBF	
ρ/a	w^{adim}	M_{xx}^{adim}	w^{adim}	M_{xx}^{adim}
0.00	0.01563	0.08125	0.01563	0.08126
0.25	0.01373	0.06836	0.01373	0.06836
0.50	0.00879	0.02969	0.00879	0.02968
0.75	0.00299	−0.03477	0.00299	−0.03479
1.00	0.0	−0.12500	0.0	−0.12498

presented an exact solution in the form

$$w(\rho,\theta)=\frac{pa^4}{64D}(a^2-\rho^2) \tag{34}$$

$$M_{\rho\rho}=\frac{p}{16}[a^2(1+\nu)-\rho^2(3+\nu)] \tag{35}$$

$$M_{\theta\theta}=\frac{p}{16}[a^2(1+\nu)-\rho^2(1+3\nu)] \tag{36}$$

In Table V the deflection and the bending moment at points at different distances from the centre are presented together with the exact results. Similar table is shown in Jin *et al.* [33] with a very good agreement as well. The present results were obtained for $N=11$ corresponding to 169 equations.

To further illustrate the results obtained the deformed shape is represented in Figure 19 and the twisting moment is shown in Figure 20.

7.6. Simply supported circular plate under uniform load

Consider the same plate as before but assuming now that it is simply supported.

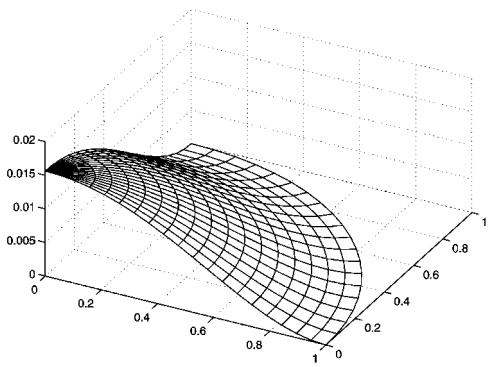

Figure 19. Clamped circular plate under uniform load: deformed shape.

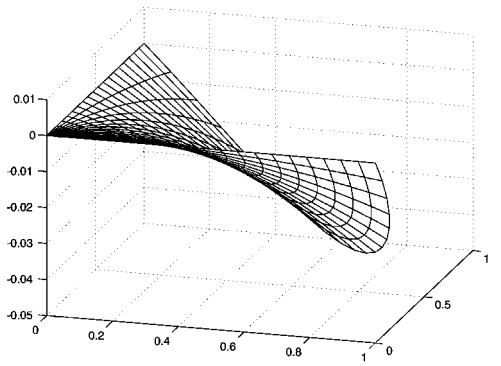

Figure 20. Clamped circular plate under uniform load: twisting moment.

Table VI. Simply supported circular plate under uniform load.

	Exact		RBF	
ρ/a	w^{adim}	M_{xx}^{adim}	w^{adim}	M_{xx}^{adim}
0.00	0.06370	0.20625	0.06369	0.20624
0.25	0.05881	0.19336	0.05880	0.19335
0.50	0.04485	0.15469	0.04484	0.15466
0.75	0.02402	0.09023	0.02402	0.09020
1.00	0.0	0.0	0.0	0.0

The exact solution is now:

$$w(\rho,\theta)=\frac{p(a^2-\rho^2)}{64D}\left(\frac{5+v}{1+v}a^2-\rho^2\right) \tag{37}$$

$$M_{\rho\rho}=\frac{p}{16}(3+v)(a^2-\rho^2) \tag{38}$$

$$M_{\theta\theta}=\frac{p}{16}[a^2(3+v)-\rho^2(1+3v)] \tag{39}$$

In Table VI the deflection and the bending moment at points at different distances from the centre are presented together with the exact results. The present results were obtained for $N=11$ corresponding to 169 equations.

8. CONCLUSIONS

In this work a meshless method for the analysis of bending of thin homogeneous plates was presented. This meshless method is based on the use of radial basis functions to build

an approximation of the general solution of the partial differential equations governing the Kirchhoff plate bending problem. The approximate solution to such problems is obtained by using the Hermite collocation method, that is, by matching, in an appropriate manner, the boundary conditions and the governing equations at selected points.

The formulation was assessed from the comparison of the results obtained with the present technique on a series of Kirchhoff plates and other results available in the literature. Those results suggest that the proposed formulation is sufficiently accurate even for plates supported only at the corners where behaviour is somehow a bit more difficult to appropriately model.

The main advantages of the proposed technique are its meshless character and the fact that it is conceptually simple (despite the apparent difficulties in defining the approximation, collocation is still much less complicated than weighted residuals). These features turn the formulation simple to implement and, consequently, computationally efficient. In this work, implementation was made in Matlab [36] and this has the added advantage that all the graphic capabilities of the system could be exploited straightforwardly.

There are many aspects of the use of RBF and Hermite collocation for Kirchhoff plates to be addressed and further developed. In the near future, efforts will be directed on the study of criteria for the definition of the optimal number and position of RBF centres and collocation points so that numerical conditioning problems (that may occur when the degree of the approximation increases unreasonably) are avoided in an optimal manner. Other alternatives (such as the compactly supported RBFs as mentioned before) are being investigated by other authors and many more developments are expected in the near future for the use of RBFs in engineering problems.

ACKNOWLEDGEMENTS

This work has been partially supported by ICIST (of which the author is a member) and by the program PRAXIS XXI as part of research project (2/2.1/CEG/33/94).

REFERENCES

1. Lucy LB. A numerical approach to the testing of the fission hypothesis. *The Astronomical Journal* 1977; **82**(12):1013–1024.
2. Nayroles B, Touzot G, Villon P. Generalizing the finite element method: diffuse approximation and diffuse elements. *Computational Mechanics* 1992; **10**:307–318.
3. Belytschko T, Lu YY, Gu L. Element-free Galerkin methods. *International Journal for Numerical Methods in Engineering* 1994; **37**:229–256.
4. Duarte CA, Oden JT. H–p clouds—an h–p meshless method. *Numerical Methods for Partial Differential Equations* 1996; **12**:673–705.
5. Babuska I, Melenk M. The partition of unity method. *International Journal for Numerical Methods in Engineering* 1997; **40**:727–758.
6. Liu WK, Li S, Belytschko T. Moving least squares reproducing kernel methods: (i) methodology and convergence. *Computational Methods in Applied Mechanics and Engineering* 1997; **143**:113–154.
7. Krongauz YV. Applications of meshless methods to solid mechanics *Ph.D. Thesis.* Northwestern University: USA, 1998.
8. Atluri SN, Zhu T. New concepts in meshless methods. *International Journal for Numerical Methods in Engineering* 2000; **47**:537–556.
9. Liu WK, Chen Y. Wavelet and multiple scale reproducing kernel methods. *International Journal for Numerical Methods in Fluids* 1995; **21**:901–931.
10. Liszka T. An interpolation method for an irregular set of nodes. *International Journal for Numerical Methods in Engineering* 1984; **20**:1599–1612.
11. Trefftz E. Ein Gegenstück zum Ritzschen Verfharen. *Proceedings of the 2nd International Cong. Applied Mechanics* 1926; 131–137.

12. Kolodziej JA. Review of application of boundary collocation methods in mechanics of continuous media. *Solid Mechanics Archives* 1987; **12**:187–321.
13. Kita E, Kamiya N. Trefftz method: an overview. *Advances in Engineering Software* 1995; **24**:3–12.
14. Leitão VMA. On a multi-region indirect Trefftz formulation for potential problems. *Engineering Analysis with Boundary Elements* 1997; **12**:77–96.
15. Leitão VMA. Application of multi-region Trefftz-collocation to fracture mechanics. *Engineering Analysis with Boundary Elements* 1998; **22**:251–256.
16. Leitão VMA, Fernandes CTT. On a multi-region Trefftz collocation method for plate bending. In *Fourth World Congress on Computational Mechanics: CD ROM Proceedings*, Idelsohn SR, Oñate E, Dvorkin EN (eds). CIMNE and IACM: Buenos Aires, Argentina, 1998.
17. Leitão VMA, Fernandes CTT. Analysis of skewed plates by a Trefftz collocation method. In *13th American Society of Civil Engineers Eng. Mech. Conference*: *CD ROM Proceedings*, Jones N, Ghanem R (eds). Johns Hopkins University: Baltimore, USA, 1999.
18. Hardy RL. Multiquadric equations of topography and other irregular surfaces. *Journal of Geophysics Res.* 1971; **176**:1905–1915.
19. Kansa EJ. Motivation for using radial basis functions to solve PDEs. 1999. http://rbf-pde.uah.edu/kansaweb.pdf, RBF-PDE Web page. http://rbf-pde.uah.edu/ [10 September 2000].
20. Fasshauer GE. Solving differential equations with radial basis functions: multilevel methods and smoothing. *Advances in Computational Mathematics* 1999; **11**(2-3):139–159.
21. Wendland H. Piecewise polynomial, positive definite and compactly supported radial basis functions of minimal degree. *Advances in Computational Mathematics* 1995; **4**:389–396.
22. Kansa EJ. Multiquadrics—a scattered data approximation scheme with applications to computational fluid-dynamics—II: Solutions to parabolic, hyperbolic and elliptic partial differential equations. *Computational Mathematics and Applications* 1990; **19**:149–161.
23. Fasshauer GE. Solving partial differential equations by collocation with radial basis functions. In *Surface Fitting and Multiresolution Methods*, LeMéhauté A, Rabut C, Shumaker L (eds). Vanderbilt University Press: Nashville, USA, 1997.
24. Wu Z. Hermite–Birkhoff interpolation of scattered data by radial basis functions. *Approximate Theory of Applications* 1992; **8**(2):1–10.
25. Franke C, Schaback R. Convergence orders of meshless collocation methods using radial basis functions. *Advances in Computational Mathematics* 1998; **93**:73–82.
26. Jumarhon B, Amini S, Chen K. The Hermite collocation method using radial basis functions. *Engineering Analysis with Boundary Elements* 2000; **24**:607–611.
27. Hon YC, Schaback R. On unsymmetric collocation by radial basis functions. *Applied Mathematics and Computers*, to appear.
28. Freitas JAT, Leitão VMA. A symmetric collocation Trefftz boundary integral formulation. *Computational Mechanics* 2000; **25**:515–523.
29. Leitão VMA. Comparison of Galerkin and collocation Trefftz formulations for plane elasticity. *Second International Workshop on the Treffitz Method*: Sintra, Portugal, 1999.
30. S. Wolfram, *Mathematica*: *A System for Doing Mathematics by Computer* (2nd edn). Addison-Wesley: Reading, MA, 1992.
31. Parreira P. On the accuracy of continuous and discontinuous boundary elements. *Engineering Analysis* 1988; **5**(4):205–211.
32. Zieliński AP, Herrera I. Trefftz method: fitting boundary conditions. *International Journal for Numerical Methods in Engineering* 1987; **24**:871–891.
33. Jin WG, Cheung YK, Zienkiewicz OC. Trefftz method for Kirchoff plate bending problems. *International Journal for Numerical Methods in Engineering* 1993; **36**(5):765–781.
34. Timoshenko SP, Woinowsky-Krieger S. *Theory of Plates and Shells* (2nd edn). McGraw-Hill: New York, 1959.
35. Jiroušek J, Leon N. A powerful finite element for plate bending. *Computer Methods in Applied Mechanics and Engineering* 1977; **12**:77–96.
36. MATLAB—The Language of Technical Computing. The MathWorks, Inc., 1999.
37. SAP2000—Structural Analysis Program. Computers and Structures, Inc., 1998.

